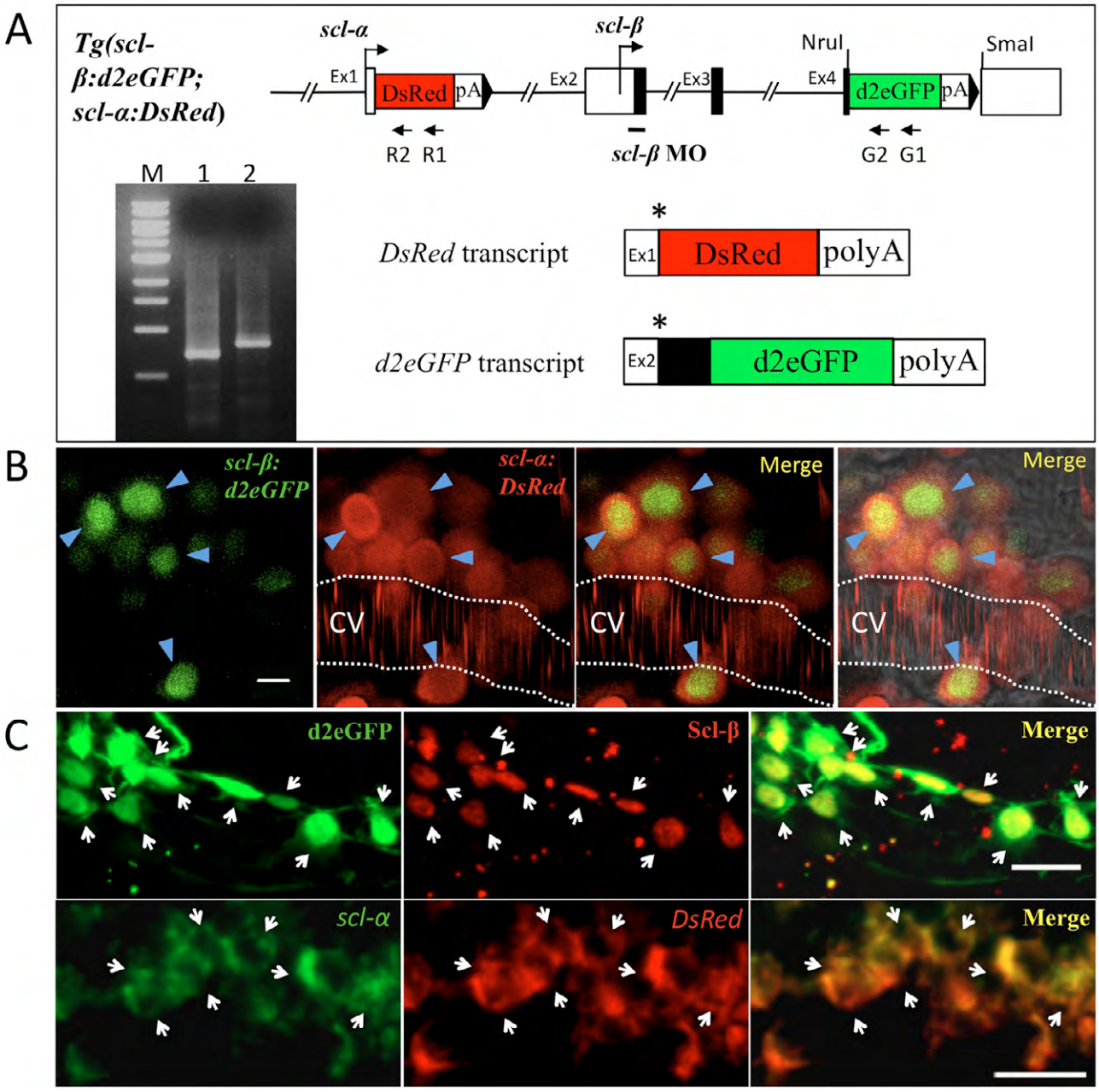

Fig. S1. The transcription and expression of d2eGFP and DsRed recapitulate that of endogenous *scl-β* and *scl-α*. (**A**) 5′-RACE experiment to determine the transcription start sites of *DsRed* and *d2eGFP*. The position of respective 5′-RACE primer set is indicated (arrows; R1 and R2 for DsRed; G1 and G2 for d2eGFP). Line 1 and line 2 show the 5′-RACE PCR products of *DsRed* and *d2eGFP*. M, 1 kb DNA ladder. The sequence result of 5′-RACE PCR products indicates that the *DsRed* transcript starts from the *scl-α* transcription initiation site and contains the non-coding exon 1, DsRed and SV40 poly(A) sequence; the *d2eGFP* transcript starts form the *scl-β* initiation site and contains the non-coding sequences of exon 2, Scl-β coding sequences of exon 2, 3 and part of exon 4 (black box), followed by the d2eGFP and SV40 poly(A) sequence. The asterisks indicate the translation initiation site of DsRed and d2eGFP, respectively. The d2eGFP protein is translated as a chimeric protein fused with the N-terminal 75 amino acids of Scl-β. (**B**) The expression of d2eGFP and DsRed in hematopoietic stem and progenitor cells in the caudal hematopoietic tissue (CHT) of 3 dpf *Tg*(*scl-β:d2eGFP; scl-α:DsRed*) larvae. D2eGFP is observed with nucleus restriction. Scale bar: 5 μm. CV, caudal vein. (**C**) Upper panel shows the double immunohistochemistry staining of d2eGFP and Scl-β (detected by Ab-Scl-C) in the anterior lateral plate mesoderm, where only Scl-β is expressed. Lower panel shows the double whole-mount *in situ* hybridization (WISH) of *DsRed* and *scl-α* (detected by *scl*-5′ probe) in the ICM of 22 hpf *Tg*(*scl-β:d2eGFP;scl-α:DsRed*) embryos. Arrows indicate the colocalized cells. Embryos are shown in lateral views with anterior to the left. Scale bars: 20 μm.

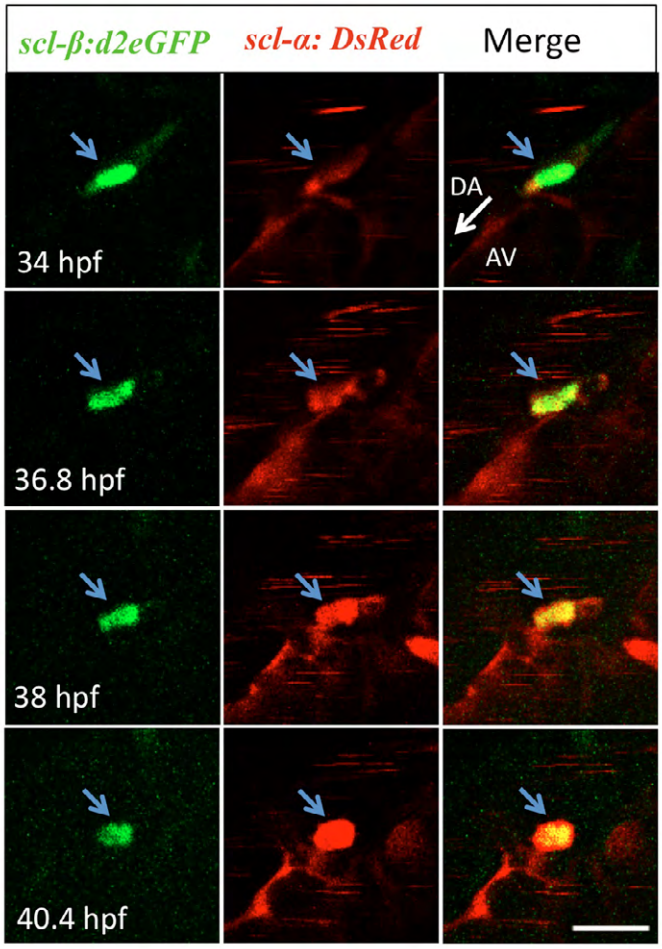

Fig. S2. *scl-β:d2eGFP*$^{+}$ endothelial cells give rise to *scl-β:d2eGFP*$^{+}$/*scl-α:DsRed*$^{+}$ HSCs. Time-lapse confocal imaging of a live *Tg*(*scl-β:d2eGFP; scl-α:DsRed*) embryo between 34 and 40 hpf. Four selected time points show the stepwise transition of an *scl-β:d2eGFP*$^{+}$ endothelial cell to an *scl-β:d2eGFP*$^{+}$/*scl-α:DsRed*$^{+}$ HSC via EHT (blue arrows). The intensity of DsRed signal is increased as the cell bends outwards. For each time point, d2eGFP, DsRed and merged images are presented. White arrow indicates the direction of circulation in DA. DA, dorsal aorta; AV, axial vein. Scale bar: 20 μm.

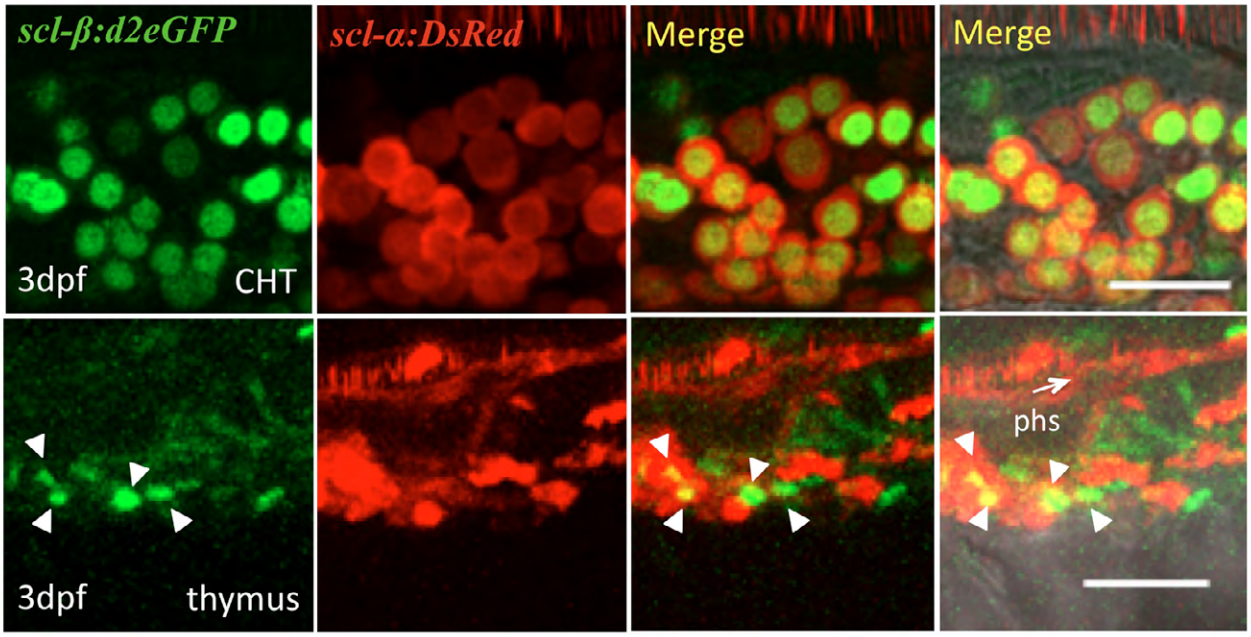

Fig. S3. *scl-β:d2eGFP*$^{+}$/*scl-α:DsRed*$^{+}$ HSCs in definitive hematopoietic tissues. Expression of *scl-β:d2eGFP* and *scl-α:DsRed* in definitive hematopoietic organs, CHT and thymus, in live *Tg*(*scl-β:d2eGFP; scl-α:DsRed*) larvae at 3 dpf. White arrowheads indicate the cells with co-expression of *scl-β:d2eGFP* and *scl-α:DsRed* in the thymus. White arrow indicates the direction of blood stream in phs. Lateral views with anterior to the left. DA, dorsal aorta; AV, axial vein; phs, primary head sinus. Scale bars: 30 μm.

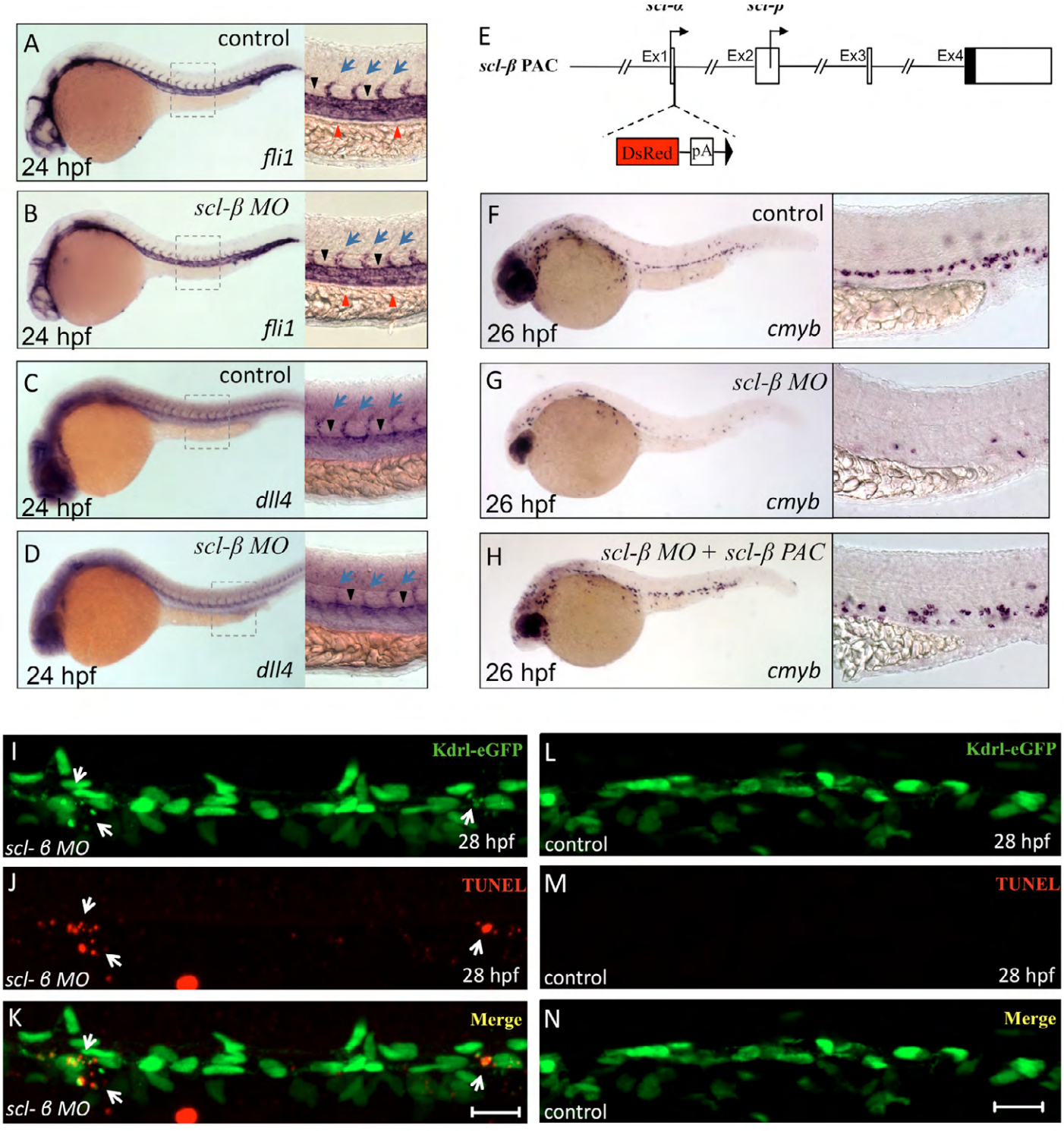

Fig. S4. ***scl-β* MO is specific to the loss of hemogenic endothelium in *scl-β* morphants.** (**A-D**) WISH of the endothelial cell-specific marker *fli1* (A,B) and artery-specific marker *dll4* (C,D) show comparable expression in control embryos and *scl-β* morphants at 24 hpf, indicating that the vascular system has developed normally in *scl-β* morphants. (**E-H**) The loss of HSCs is partially rescued in the *scl-β* morphant receiving *scl-β* PAC expression. (E) The *scl-β* PAC. DsRed and an SV40 polyadenylation signal cassette were inserted behind exon 1 to interrupt the transcription of *scl-α*, whereas the expression of *scl-β* is not affected. (F-H) WISH of the HSC-specific marker *cmyb* in the 26 hpf control embryo (F), *scl-β* morphant (G) and *scl-β* morphant injected with *scl-β* PAC (H). A lower magnification (8×) is shown to the left and a higher magnification (20×) of the trunk region to the right. Lateral views with anterior to the left. (**I-N**) Double immunostaining of Kdrl:eGFP and TUNEL in the AGM of 28 hpf *scl-β* morphants (I-K) and control embryos (L-N). White arrows indicate two Kdrl:eGFP^{+} cells undergoing apoptosis in the AGM. Scale bar: 20 μm.

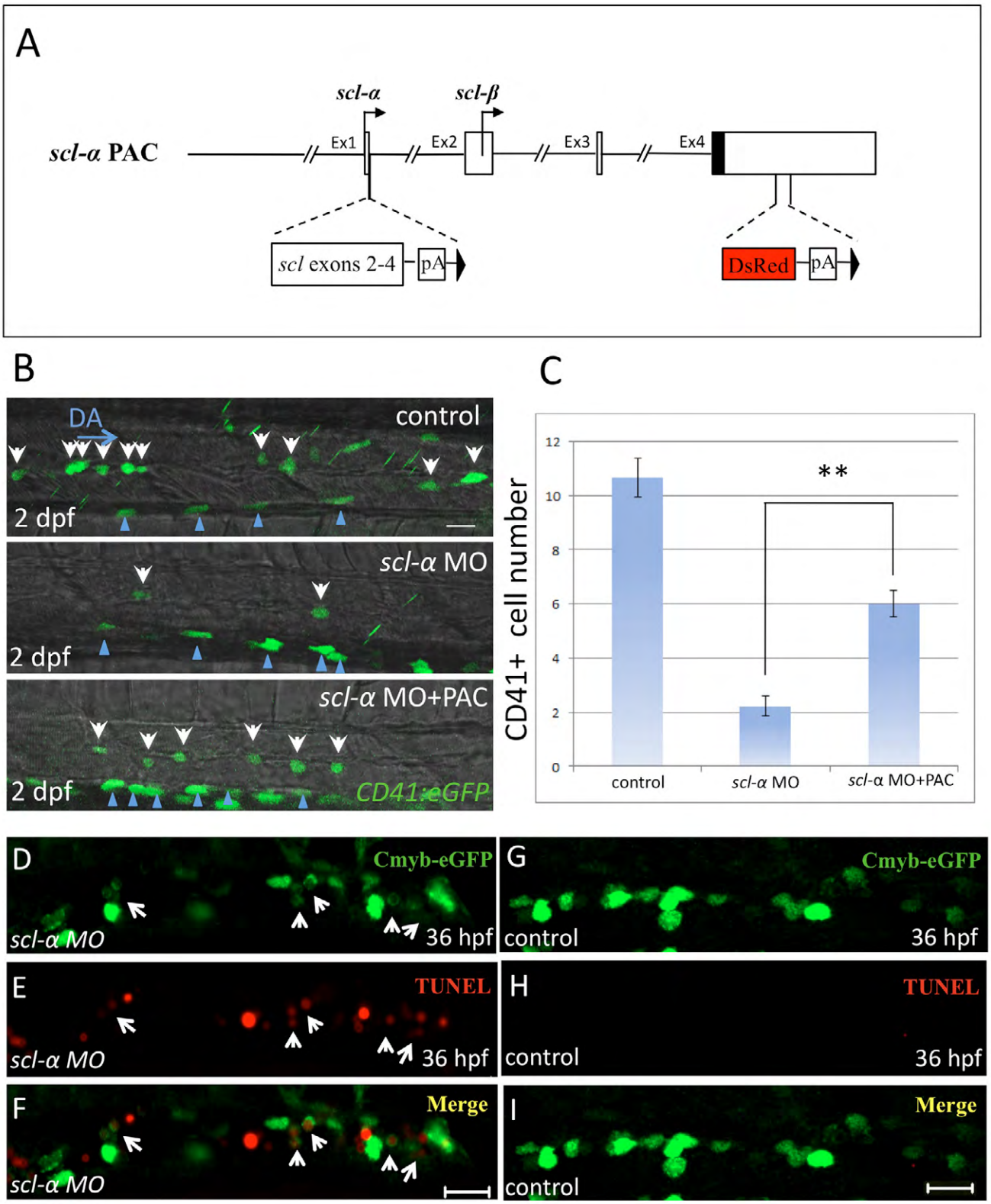

Fig. S5. *scl-α* MO is specific to the defects of HSC maintenance in the AGM of *scl-α* morphants. (**A-C**) The loss of HSCs is partially rescued in the *scl-α* morphant receiving *scl-α* PAC expression. (A) The *scl-α* PAC used for rescue. DsRed and an SV40 polyadenylation signal were inserted in exon 4 to interrupt the transcription of *scl-β*. To introduce normal expression of *scl-α*, the DNA sequences of *scl* exon 2, 3, 4 and an SV40 polyadenylation signal were inserted behind exon 1. (B) *CD41:eGFP*$^{+}$ HSCs in the AGM region of live 2 dpf control embryos, *scl-α* morphants and *scl-α* morphants injected with *scl-α* PAC. White arrows indicate *CD41:eGFP*$^{+}$ HSCs in the AGM. Blue arrowheads identify pronephric duct cells. Scale bar: 20 μm. (C) Statistical analysis showing the number of *CD41:eGFP*$^{+}$ HSCs (per five somites) in the AGM of 2 dpf control embryos, *scl-α* morphants and *scl-α* morphants injected with *scl-α* PAC. (**D-I**) Double immunostaining of Cmyb-eGFP and TUNEL in the AGM of 36 hpf *scl-α* morphants (D-F) and control embryos (G-I). White arrows indicate three Cmyb:eGFP^{+} cells undergoing apoptosis in the AGM. Scale bar: 20 μm.

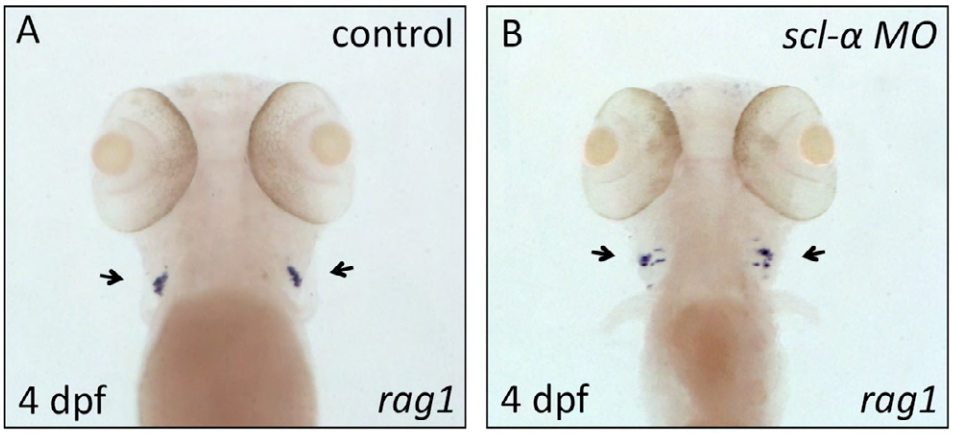

Fig. S6. T-cell development is viable in *scl-α* morphants. WISH of the T lymphocyte-specific marker *rag1* (black arrows) in 4 dpf control embryos (**A**) and *scl-α* morphants (**B**) shows that T-cell development is viable in the thymus of *scl-α* morphants. Dorsal views, anterior up.

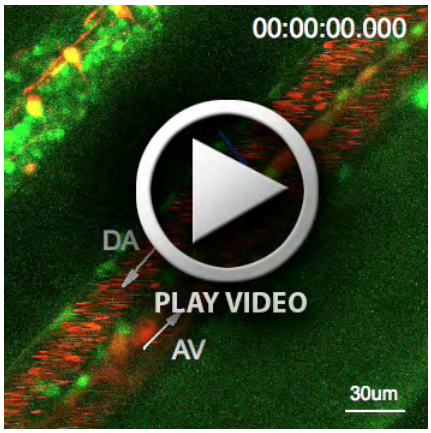

Movie 1. Motility of *scl-β:d2eGFP*$^{+}$/*scl-α:DsRed*$^{+}$ HSCs in the AGM. Time-lapse confocal imaging of the DA and AV region of a live *Tg*(*scl-β:d2eGFP; scl-α:DsRed*) embryo from 36 to 70 hpf. The *scl-β:d2eGFP*$^{+}$/*scl-α:DsRed*$^{+}$ HSCs show high motility in the AGM: they move around within the space between the DA and AV, undergo cell division, and enter circulation through the AV. Time is indicated in hours, minutes and seconds in the upper right corner of each movie.

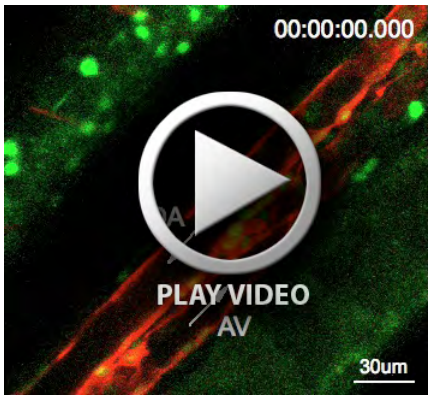

Movie 2. Expression of *scl-β:d2eGFP* in VAE cells correlates with EHT. Time-lapse confocal imaging of the DA and AV region of a live *Tg*(*scl-β:d2eGFP; kdrl:Ras-mCherry*) embryo from 30 to 43 hpf. Arrows and numbers indicate that *scl-β:d2eGFP*$^{+}$/*kdrl:Ras-mcherry*$^{+}$ cells bud from the floor of the DA towards the AV, transform to round cells and remain in the region between the DA and AV, and finally enter circulation through the AV. Selected images are also shown in Fig. 3B-K.

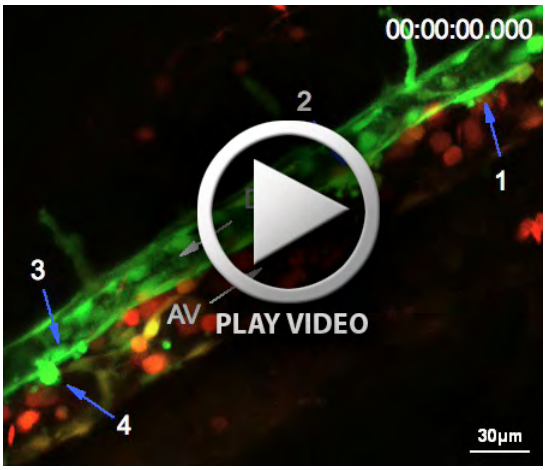

Movie 3. *scl-β* deficiency inhibits HSC formation by depleting the hemogenic endothelium. Time-lapse confocal imaging of the DA and AV region of a live *Tg*(*scl-α:DsRed; kdrl:eGFP*) embryo injected with *scl-β* MO (morphants) from 25 to 35 hpf. Arrows and numbers identify some *kdrl:eGFP*$^{+}$ ventral aortic endothelial cells that burst into fragments before apparent signs of EHT. Concomitantly, these *kdrl:eGFP*$^{+}$ VAE cells have no obvious expression of *scl-α:DsRed.* As a result, there are no *scl-α:DsRed*$^{+}$/*kdrl:eGFP*$^{+}$ HSCs formed in the AGM region of the transgenic *scl-β* morphant. Selected images are also shown in Fig. 4B-D″. As the embryo grows, the circulating red blood cells (*scl-α:DsRed*$^{+}$) become clear and are seen as stripes in vessels due to the rapid confocal scanning.

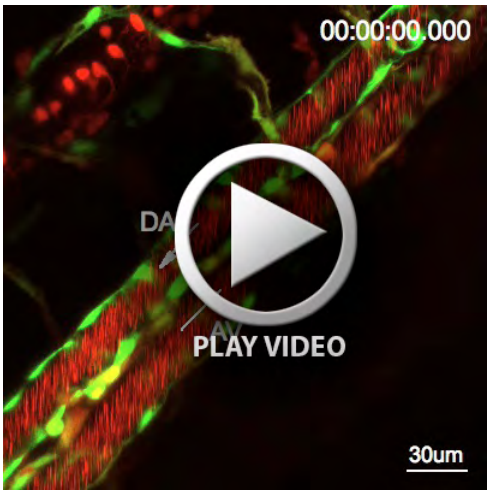

Movie 4. *scl-α* deficiency inhibits the maintenance of HSCs in the AGM. Time-lapse confocal imaging of the DA and AV region of a live *Tg*(*scl-α:DsRed; kdrl:eGFP*) embryo injected with *scl-α* MO (morphants) from 37 to 50 hpf. The *scl-α:DsRed*$^{+}$/*kdrl:eGFP*$^{+}$ HSCs are formed normally and remain in the AGM region. Arrows and numbers indicate the HSCs that undergo fragmentation. Selected images are also shown in Fig. 6J-L″.

Movie 5. *runx1* is required for successful budding of HSCs from endothelial cells. Time-lapse confocal imaging of the DA and AV region of a live *Tg*(*scl-α:DsRed; kdrl:eGFP*) embryo injected with *runx1* MO (morphants) from 30 to 37 hpf. Arrows and numbers indicate the *kdrl:eGFP*$^{+}$ ventral aortic endothelial cells that tend to bud towards the AV, with increasing expression of *scl-α:DsRed*, but finally burst into small fragments. Selected images are also shown in Fig. 7C-E″.

Table S1. Quantification of *scl-β:d2eGFP*$^{+}$ endothelial cells and EHT events observed in six *Tg*(*scl-β:d2eGFP; kdrl:Ras-mCherry*) embryos from 28 to 60 hpf

Embryo No.	Number of observed *scl-β:d2eGFP*$^{+}$ endothelial cells	Number of observed *scl-β:d2eGFP*$^{+}$ endothelial cells undergoing EHT	Number of observed *scl-β:d2eGFP*$^{–}$ endothelial cells undergoing EHT
1	13	10	0
2	11	8	0
3	7	4	0
4	10	9	0
5	8	6	0
6	11	9	0

Table S2. Quantification of *scl-α:DsRed*-expressing cells and EHT events observed in four *Tg*(*scl-α:DsRed; kdrl:eGFP*) embryos from 30 to 60 hpf

Embryo No.	Number of EHT events with *scl-α:DsRed* expression in correlating endothelial cells	Number of EHT events without *scl-α:DsRed* expression in correlating endothelial cells
1	11	0
2	6	0
3	8	0
4	9	0